

Near-infrared spectroscopy assessment of cerebral oxygen metabolism in the developing premature brain

Nadège Roche-Labarbe¹, Angela Fenoglio², Alpna Aggarwal³, Mathieu Dehaes², Stefan A Carp¹, Maria Angela Franceschini¹ and Patricia Ellen Grant^{2,3}

¹Athinoula A Martinos Center for Biomedical Imaging, Massachusetts General Hospital/Harvard Medical School, Charlestown, Massachusetts, USA; ²Fetal-Neonatal Neuroimaging and Developmental Science Center, Children's Hospital Boston, Boston, Massachusetts, USA; ³Division of Newborn Medicine, Children's Hospital, Boston, Massachusetts, USA

Little is known about cerebral blood flow, cerebral blood volume (CBV), oxygenation, and oxygen consumption in the premature newborn brain. We combined quantitative frequency-domain near-infrared spectroscopy measures of cerebral hemoglobin oxygenation (SO₂) and CBV with diffusion correlation spectroscopy measures of cerebral blood flow index (BF_{ix}) to determine the relationship between these measures, gestational age at birth (GA), and chronological age. We followed 56 neonates of various GA once a week during their hospital stay. We provide absolute values of SO₂ and CBV, relative values of BF_{ix}, and relative cerebral metabolic rate of oxygen (rCMRO₂) as a function of postmenstrual age (PMA) and chronological age for four GA groups. SO₂ correlates with chronological age ($r = -0.54$, P value ≤ 0.001) but not with PMA ($r = -0.07$), whereas BF_{ix} and rCMRO₂ correlate better with PMA ($r = 0.37$ and 0.43 , respectively, P value ≤ 0.001). Relative CMRO₂ during the first month of life is lower when GA is lower. Blood flow index and rCMRO₂ are more accurate biomarkers of the brain development than SO₂ in the premature newborns.

Journal of Cerebral Blood Flow & Metabolism (2012) 32, 481–488; doi:10.1038/jcbfm.2011.145; published online 26 October 2011

Keywords: brain hemodynamic development; cerebral oxygen consumption; diffuse correlation spectroscopy; frequency-domain near-infrared spectroscopy; premature neonates

Introduction

Premature birth interferes with normal brain maturation, and clinical events and interventions may have additional deleterious effects. Compared with normal term newborns, premature newborns at term equivalent postmenstrual age (PMA) have structural abnormalities on magnetic resonance imaging (Huppi *et al*, 1998) and magnetic resonance diffusion abnormalities that have been associated with functional impairment (Bassi *et al*, 2008), and their resting state functional connectivity networks are abnormal (Smyser *et al*, 2010). Using near-infrared

spectroscopy (NIRS), several studies have described alterations in cerebral blood volume (CBV) and oxygenation in preterm newborns (see review in Wolf and Greisen, 2009). However, little is known about baseline cerebral blood flow, oxygenation, and oxygen consumption in the premature newborn's brain. Such information, especially if available at the bedside, would provide valuable insight on early brain development and the impact of premature birth.

Near-infrared spectroscopy is a portable and noninvasive method for interrogating cerebral physiology that uses low-intensity nonionizing radiation. It is thus suitable for use in neonates, whose thin scalps and skulls facilitate light transmission. Contrary to continuous wave NIRS measures of changes in oxy- and deoxy-hemoglobin concentrations (respectively, HbO (oxygenated hemoglobin concentration) and HbR (reduced hemoglobin concentration)) (Wolf and Greisen, 2009; Wyatt *et al*, 1986), frequency-domain near-infrared spectroscopy (FDNIRS) provides absolute values of HbO and HbR from which absolute values of CBV and hemoglobin oxygen saturation (SO₂) can be calculated (Fantini *et al*, 1995; Zhao *et al*, 2005). Frequency-domain

Correspondence: Dr N Roche-Labarbe, Athinoula A Martinos Center for Biomedical Imaging, Massachusetts General Hospital, Building 149, 13th Street, Charlestown MA 02129, USA.

E-mail: nadege@nmr.mgh.harvard.edu

This work was supported by NIH Grant R01 HD042908, P41-RR14075, and R21-HD058725 and by Clinical Translational Science Award UL1RR025758 to Harvard University and Brigham and Women's Hospital from the National Center for Research Resources.

Received 2 June 2011; revised 1 September 2011; accepted 7 September 2011; published online 26 October 2011

near-infrared spectroscopy has been successful in measuring the evolution of CBV, SO_2 , and relative cerebral metabolic rate of oxygen ($rCMRO_2$) over the first year of normal brain development (Franceschini *et al*, 2007), establishing baseline values of CBV, SO_2 , and $rCMRO_2$ during the first 6 weeks of life in premature neonates (Roche-Labarbe *et al*, 2010), and determining the effect of acute brain injury on these parameters (Grant *et al*, 2009).

Diffusion correlation spectroscopy (DCS) provides a measure of tissue perfusion based on the movement of scatterers (i.e., blood cells) inside the tissue (Boas and Yodh, 1997; Cheung *et al*, 2001). Diffusion correlation spectroscopy is a valid assessment of cerebral blood flow changes in the adult brain (Durduran *et al*, 2004; Li *et al*, 2005) and infants (Buckley *et al*, 2009; Durduran *et al*, 2010; Roche-Labarbe *et al*, 2010) and a safe and reliable alternative to the oxygen bolus (Edwards *et al*, 1988) or indocyanine green (Patel *et al*, 1998) methods.

Combining FDNIRS measures of CBV and SO_2 and DCS measures of blood flow index (BF_{ix}) allows for reliable calculation of local $rCMRO_2$ in the newborns (Roche-Labarbe *et al*, 2010). Quantification will improve estimation of normal values and detection of abnormalities in at-risk neonates (Nicklin *et al*, 2003). Such markers of brain development and detection of deviations from normal can be obtained before the age at which accurate behavioral and neurologic assessments can be performed, potentially providing early biomarkers for adverse outcomes.

Here, we studied premature neonates with no known brain injury to determine the relationship between CBV, SO_2 , $rCMRO_2$, and BF_{ix} , gestational age (GA) and chronological age.

Materials and methods

Subjects

We studied 56 neonates (24 to 37 weeks GA at birth, 25 females) enrolled from the neonatal intensive care units and Well Baby Nurseries at the Massachusetts General Hospital, Brigham and Women's Hospital and Children's Hospital Boston between 2008 and 2010. Subjects were included if they had no diagnosis of brain injury or neurologic issue during or after their hospital stay. They were sorted into four groups: 24 to 27 weeks GA (9 subjects, 55 measurements, 6 ± 3 measurements per infant, APGAR score at 5 minutes = 8 ± 0.5 , weight at birth = 930 ± 180 g), 28 to 30 weeks GA (10 subjects, 65 measurements, 7 ± 1 measurements per infant, APGAR score at 5 minutes = 7.4 ± 0.7 , weight at birth = $1,200 \pm 350$ g), 31 to 33 weeks GA (18 subjects, 64 measurements, 4 ± 1 measurements per infant, APGAR score at 5 minutes = 8.5 ± 0.6 , weight at birth = $1,730 \pm 300$ g) and 34 to 37 weeks GA (19 subjects, 44 measurements, 2 ± 1 measurements per infant, APGAR score at 5 minutes = 8.4 ± 1 , weight at birth = $2,180 \pm 250$ g). Subjects included had a variety of cardiovascular and respiratory conditions representative of the neonatal intensive care unit population (Supplementary Table 1). Each infant was measured once

a week from 1 to 15 weeks of age (ages in days were rounded off to the nearest week) while in the hospital. Our Institutional Review Board, the Partners Human Research Committee, approved all the aspects of this study and all parents provided informed consent.

Acquisition

We used a customized FDNIRS instrument from ISS Inc., Champaign, IL, USA (<http://www.iss.com/products/oxi-plex/>), and built a DCS instrument similar to the system developed by Drs Arjun Yodh and Turgut Durduran at the University of Pennsylvania (Carp *et al*, 2010; Cheung *et al*, 2001; Durduran *et al*, 2004). Both instruments are described in detail in Roche-Labarbe *et al* (2010).

The FDNIRS sources and detector fiber bundles (each 2.5 mm diameter) were arranged in a row in a black rubber probe ($5 \times 2 \times 0.5$ cm³) with source-detector distances of 1, 1.5, 2, and 2.5 cm (Figure 1C), adequate for a depth penetration of ~ 1 cm, which includes the cerebral cortex in neonates (Dehaes *et al*, 2011; Franceschini *et al*, 1998). The DCS laser (50 mW power) was coupled to a 62.5- μ m diameter multimode optical fiber and diffused at the fiber tip to comply with the American National Standards Institute exposure standards. The detectors were coupled to 5.6- μ m single mode optical fibers. The DCS fibers were arranged in a second row parallel to the NIRS bundles, with source-detector distances of 1.5 (one fiber) and 2 cm (three fibers) (Figure 1C). For each measurement, the probe and fibers were placed in a single-use polypropylene sleeve for hygiene reasons (Figure 1A).

Frequency-domain near-infrared spectroscopy and DCS measurements were obtained in sequence from seven areas of the head (Figure 1B). The optical probe was held in each location for up to three times 10 seconds of data acquisition. Repositioning the probe compensated for local inhomogeneities such as hair and superficial large vessels to ensure that the measurement was representative of the

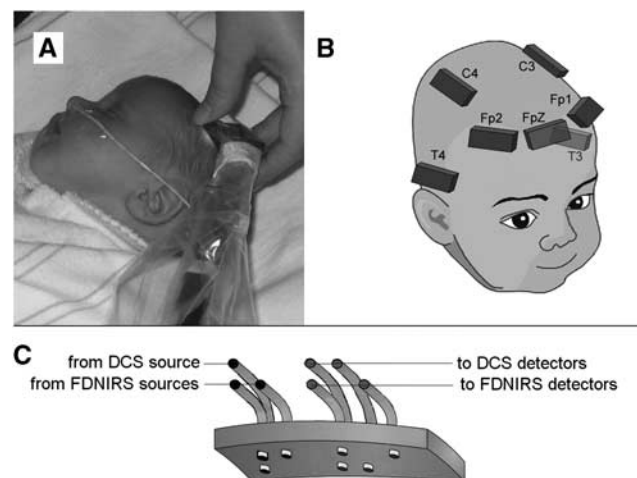


Figure 1 (A) Subject during a measurement. (B) Locations of recording on the subject's head. (C) Schema of the probe. DCS, diffusion correlation spectroscopy; FDNIRS, frequency-domain near-infrared spectroscopy.

underlying brain region. The total number of positions and repetitions depended on the cooperation of the subject and the presence of other medical devices on the head. Total examination time was ~45 minutes. Hemoglobin counts were extracted from clinical reports and arterial oxygenation (SaO₂) was obtained from routine monitors at the time of the measurement session.

Near-Infrared Spectroscopy Data Processing

Amplitude and phase data collected at each wavelength allows the calculation of average absorption and scattering coefficients using the multidistance frequency-domain method (Fantini *et al*, 1995). An automated data analysis routine includes data quality assessment and data rejection based on previously established statistical criteria (Roche-Labarbe *et al*, 2010). Oxygenated hemoglobin concentration and HbR were derived by fitting the absorption coefficient at our wavelengths with the hemoglobin spectra using the extinction coefficients reported in the literature (Wray *et al*, 1988) and a 75% concentration of water (Wolthuis *et al*, 2001). Total hemoglobin concentration HbT = HbO + HbR (μmol) and SO₂ = HbO/HbT (%). Cerebral blood volume in mL/100 g was calculated using standard equations (Franceschini *et al*, 2007; Takahashi *et al*, 1999) and hemoglobin concentration in the blood (HGB) from clinical charts. For 20% of measurements, HGB was not available, in which case standard normal values for HGB for age were used (de Alarcón and Werner, 2005).

Diffusion Correlation Spectroscopy Data Processing

Diffusion correlation spectroscopy data comprise a set of intensity autocorrelation curves (over a delay time range of 200 nanoseconds ~1 second in our case) acquired sequentially at 1 Hz. Following the diffusion correlation equations (Boas and Yodh, 1997; Cheung *et al*, 2001; Culver *et al*, 2003; Durduran *et al*, 2004), a BF_{ix} was derived fitting the normalized intensity temporal autocorrelation profile of the diffusively reflected light to the measured temporal autocorrelation function (Boas *et al*, 1995; Boas and Yodh, 1997; Cheung *et al*, 2001). To maximize accuracy, we used the actual optical absorption and scattering coefficients at 785 nm interpolated from the FDNIRS measurements. We rejected measurements that do not met objective criteria (Roche-Labarbe *et al*, 2010).

Relative CMRO₂ from combined DCS and FDNIRS measures was calculated as the ratio between the subject's values and the average of all the first week's values (indicated by the subscript 0) of the 34 to 37 weeks GA group using the following equation:

$$\text{rCMRO}_2 = \frac{\text{CMRO}_2}{\text{CMRO}_{20}} = \frac{\text{HGB}}{\text{HGB}_0} \cdot \frac{\text{BF}_{ix}}{\text{BF}_{ix0}} \cdot \frac{\text{SaO}_2 - \text{SO}_2}{\text{SaO}_{20} - \text{SO}_{20}}$$

Statistical analysis

In each infant for each measurement session and for each measured parameter (HbO, HbR, HbT, SO₂, CBV, BF_{ix}, and

rCMRO₂), results were averaged over all positions. We verified that results are consistent when only one location is considered. We averaged data sets to obtain one time point per week (ages in days were rounded off to the nearest week, for example, 3 days becomes week 0, 12 days becomes week 2). Given our small sample size, confidence intervals were calculated using Student's tables.

We calculated linear regression, correlation coefficients (*r*), coefficient of determination (*R*²), and significance levels between each measured parameter and HGB, chronological age, or PMA for all time points. Finally, we calculated linear regression between each measured parameter and chronological age for the first 31 days of life (4.4 weeks), then between each measured parameter and PMA for time points taken between 34 and 38.4 weeks PMA. These periods correspond to the overlapping measurements among all four groups. We performed *t*-tests for independent subjects with Bonferroni adjustment of significance levels on the slopes and intercepts (for each element in Table 2; *i.e.*, 42 elements).

Results

Figure 2 illustrates the weekly average of FDNIRS/DCS measured and derived parameters as a function of age for the four GA groups with confidence intervals. Figure 3 illustrates the same parameters as a function of PMA. For the four GA groups, Figure 2 shows that HbO, HbT, and SO₂ decrease with chronological age, HbR and CBV are constant with age, and BF_{ix} and rCMRO₂ increase with age. Figure 3 shows that the decrease in HbO, HbT, and SO₂ of the four groups is independent of PMA, while the increase in BF_{ix} and rCMRO₂ is associated with PMA (scatterplots of individual measurements as Supplementary Figures 1 and 2).

Table 1 presents the results of linear regressions of the measured and derived optical parameters with HGB, age, and PMA across groups at all time points. To specifically illustrate differences among groups, Table 2 presents the results of the *t*-test on slopes and intercepts of the measured and derived parameters during the first month of life. Differences in slope, as seen on SO₂, reflect different rates of progression between GA groups, while differences in intercepts for similar slopes, as seen on rCMRO₂, reflect different absolute values between GA groups. Because the differences in CBV intercepts are due to the large variance in the 24 to 27 group in the first weeks of life (Figure 2), which is confirmed by the absence of correlation with any factor (Table 1), they do not reflect true intergroup differences. *t*-Test on slopes and intercepts between groups at same PMA showed no significant or near significant differences. Figure 4 represents the trends (slopes and intercepts) of SO₂ and rCMRO₂ maturation during the first month of life as a function of GA at birth (other box plots as Supplementary Figure 3). SO₂ decrease is steeper and occurs at an earlier PMA in subjects born at a lower GA (slopes are different). Relative CMRO₂

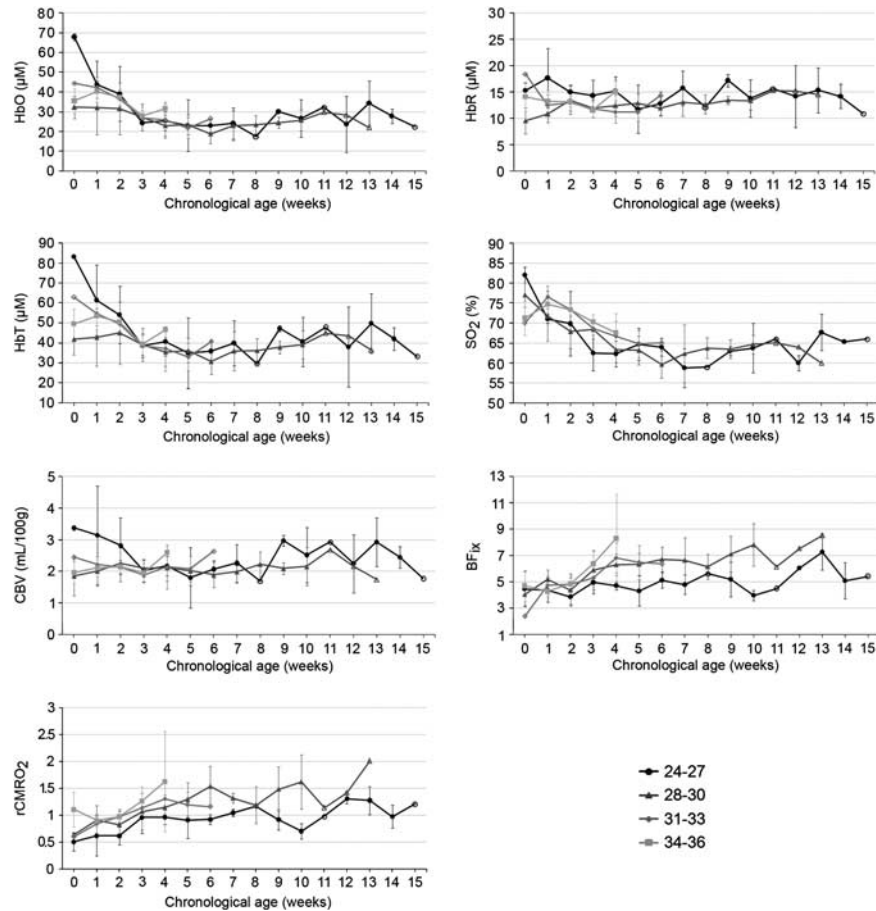


Figure 2 Measured and derived parameters as a function of chronological age. Confidence intervals are displayed where two or more values were averaged. Filled markers were used when at least two values were averaged, empty markers represent individual values. BF_{ix}, blood flow index; CBV, cerebral blood volume; HbO, oxygenated hemoglobin concentration; HbR, reduced hemoglobin concentration; HbT, total hemoglobin concentration; rCMRO₂, relative cerebral metabolic rate of oxygen; SO₂, oxygen saturation.

during the first month of life is proportional to GA at birth (slopes are comparable but intercepts are proportional to GA).

Discussion

We (1) provided absolute values of HbO, HbR, HbT, SO₂, and CBV and relative values of BF_{ix} and rCMRO₂ as a function of gestational and chronological age; (2) found that SO₂ correlates with chronological age but not with PMA; (3) BF_{ix} and rCMRO₂ correlate better with PMA than with chronological age; and (4) rCMRO₂ during the first month of life is lower when GA at birth is lower.

SO₂ is not correlated with PMA but varies with chronological age and HGB, suggesting that it depends on systemic changes and does not reflect changes associated with brain development. This is consistent with the findings that SO₂ correlates with the heart and respiratory rate and with arterial SO₂ in newborns (Tina *et al*, 2009). SO₂ undergoes a dip around 6 to 8 weeks of life, probably due to the

transition from fetal to adult hemoglobin (Franceschini *et al*, 2007; Roche-Labarbe *et al*, 2010). This decrease is steeper and occurs at an earlier PMA in subjects born at a lower GA. This is because SO₂ immediately after birth is higher when GA is lower (Tina *et al*, 2009), and because SO₂ is highly dependent on HGB, which starts decreasing at birth regardless of GA and decreases faster in more premature infants (de Alarcón and Werner, 2005). These findings question the relevance of SO₂ as a measure of brain health and brain development in newborns, and are consistent with the results showing that SO₂ is not sensitive to evolving acute brain injury in newborns (Grant *et al*, 2009). The focus on SO₂ may explain why many early NIRS studies yielded inconsistent results, which hampered the implementation of NIRS in clinical settings (Greisen, 2006; Nicklin *et al*, 2003). Those using NIRS to evaluate hemodynamics in infants have typically used SO₂ rather than other parameters, and SO₂ is sensitive to transient hemodynamic changes (Huang *et al*, 2004; Naulaers *et al*, 2004; Petrova and Mehta, 2006; Toet *et al*, 2005). However, SO₂ is the

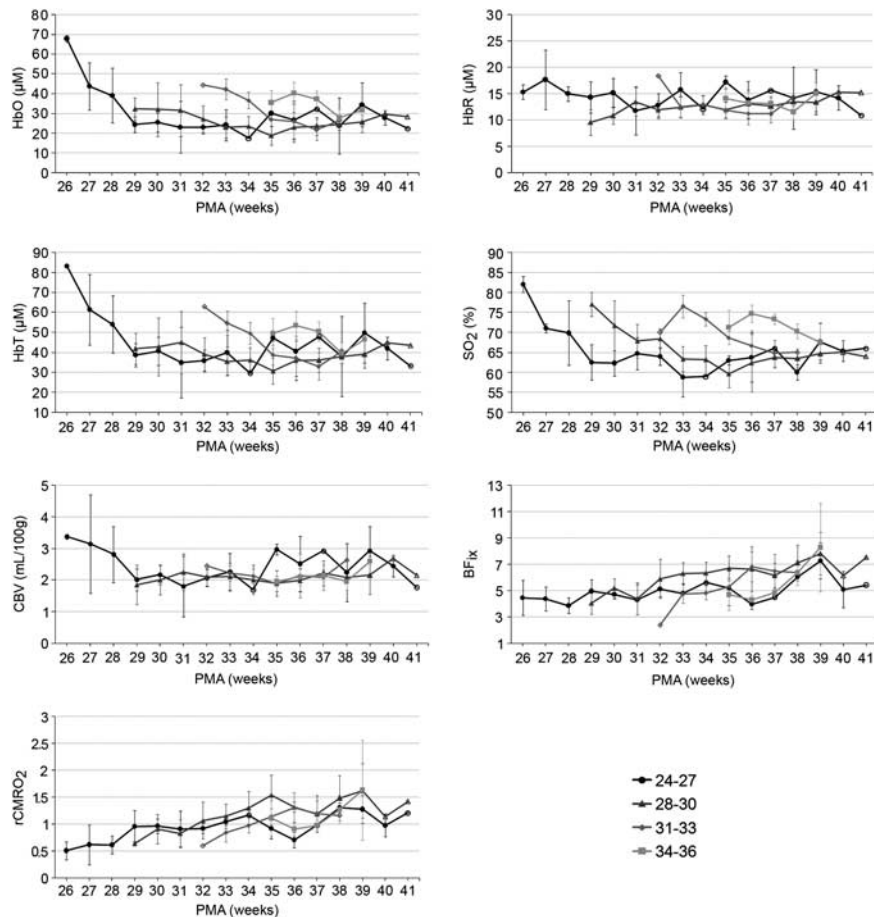


Figure 3 Measured and derived parameters as a function of postmenstrual age (PMA). Postmenstrual age for each group is calculated starting from the group's median gestational age (GA). Confidence intervals are displayed where two or more values were averaged. Filled markers were used when at least two values were averaged, empty markers represent individual values. BF_{ix}, blood flow index; CBV, cerebral blood volume; HbO, oxygenated hemoglobin concentration; HbR, reduced hemoglobin concentration; HbT, total hemoglobin concentration; rCMRO₂, relative cerebral metabolic rate of oxygen; SO₂, oxygen saturation.

Table 1 Correlation coefficient and significance (*) in individual measurements

	HGB	Chronological age	PMA
HbO	0.55***	-0.39***	-0.13
HbR	0.02	0.10	-0.05
HbT	0.48***	-0.32***	-0.12
SO ₂	0.66***	-0.54***	-0.07
CBV	-0.12	0.07	-0.10
BF _{ix}	-0.38***	0.35***	0.37***
rCMRO ₂	-0.19**	0.31***	0.43***

BF_{ix}, blood flow index; CBV, cerebral blood volume; HbO, oxygenated hemoglobin concentration; HbR, reduced hemoglobin concentration; HbT, total hemoglobin concentration; HGB, hemoglobin blood count; PMA, postmenstrual age; rCMRO₂, relative cerebral metabolic rate of oxygen; SO₂, oxygen saturation.

Significance legend: *P value ≤0.05; **P value ≤0.01; ***P value ≤0.001.

parameter least sensitive to development or the evolution of injury.

Blood flow index and rCMRO₂ correlate better with PMA and are less dependent on chronological

age than SO₂, suggesting that they are more sensitive to hemodynamic and metabolic changes associated with early brain development. Relative CMRO₂ during the first month of life is proportional to GA at birth, which is consistent with the correlation between GA at birth and spontaneous neuronal activity transients measured with electrophysiology (André *et al*, 2010). This is also consistent with the findings that fractional tissue oxygen extraction during the first 6 hours of life is higher when GA at birth is higher (Tina *et al*, 2009).

When subjects from various GA groups increase in chronological age, rCMRO₂ shows an increase over time, which may reflect increasing oxygen requirements due to synaptic development. We did not find rCMRO₂ differences between GA groups at the same PMA, suggesting that synaptic production is appropriate for PMA, regardless of GA at birth. This is consistent with primate studies showing that premature birth does not affect the rate of synaptic production in the visual cortex: synaptogenesis correlates with PMA but not chronological age despite increased sensory stimulation (Bourgeois

Table 2 *t*-Tests on slopes and intercepts for the first month of life

	HbR	HbO	HbT	SO ₂	CBV	BF _{ix}	rCMRO ₂
(A) Slopes							
24–27 versus 28–30	–	–	–	–	–	–	–
24–27 versus 31–33	–	+	+	+	+	–	–
24–27 versus 34–36	–	–	–	*	–	–	–
28–30 versus 31–33	–	–	–	–	–	–	–
28–30 versus 34–36	–	–	–	+	–	–	–
31–33 versus 34–36	–	–	–	*	–	–	*
(B) Intercepts							
24–27 versus 28–30	*	+	+	–	+	–	–
24–27 versus 31–33	+	+	*	–	*	–	–
24–27 versus 34–36	–	+	–	+	*	–	*
28–30 versus 31–33	–	–	–	–	–	–	–
28–30 versus 34–36	–	–	–	–	–	–	+
31–33 versus 34–36	–	–	–	+	–	–	+

BF_{ix}, blood flow index; CBV, cerebral blood volume; HbO, oxygenated hemoglobin concentration; HbR, reduced hemoglobin concentration; HbT, total hemoglobin concentration; rCMRO₂, relative cerebral metabolic rate of oxygen; SO₂, oxygen saturation.

–*P* value ≥ 0.055; +*P* value < 0.055 (near significant); **P* value < 0.05 (significant, Bonferroni corrected).

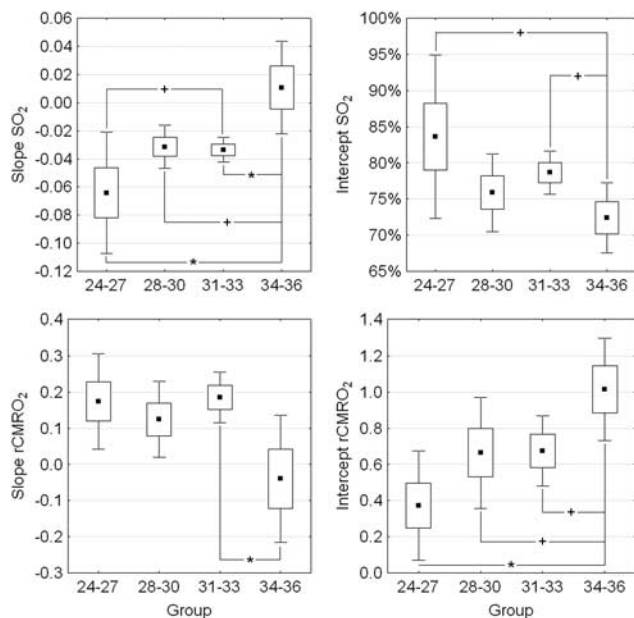


Figure 4 Boxplots of slope and intercept of oxygen saturation (SO₂) and relative cerebral metabolic rate of oxygen (rCMRO₂) during the first month of life. The dot is the mean, the box is the standard error, the whiskers depict the 0.95 confidence interval. Legend: + *P* value < 0.055 (near significant); * *P* value < 0.05 (significant, Bonferroni corrected).

et al, 1989). The consistency of rCMRO₂ with PMA regardless of GA is also consistent with angiogenesis being driven by intrinsic mechanisms associated with synaptogenesis, with no direct effect of outside stimulation (Fonta and Imbert, 2002). However, it

conflicts with reports of thinner cortex associated with premature birth (Nagy *et al*, 2010).

Slopes of BF_{ix} were similar among GA groups, but so were intercepts, perhaps due to competitive influences of HGB decreasing (BF_{ix} was more influenced by HGB than rCMRO₂) and neuronal activity increasing BF_{ix}. Overall, these results that agree with the findings in brain-injured neonates (Grant *et al*, 2009), suggest that rCMRO₂ is a better indicator of brain health and developmental stage in infants than SO₂.

Oxygenated hemoglobin concentration, HbR, and HbT constitute the output of most NIRS systems and are provided for comparison purposes. Cerebral blood volume does not show any consistent behavior during the first weeks of life (Franceschini *et al*, 2007; Roche-Labarbe *et al*, 2010). Cerebral blood volume was higher in the 24 to 27 group compared with the other groups during the first 3 weeks of life (different intercepts), but the large variance in that group and the absence of correlation with any factor (HGB, age, or PMA) suggests that this may be an artifact due to small sample size in that group at that age.

Because premature infants are often treated with medication or require respiratory assistance, we included them in analyses. The variety of cardiac and respiratory conditions among subjects probably contributed to the intragroup variability, particularly in the lower GA group. Caffeine, commonly administered to premature infants with apnea, stimulates neurons and decreases cerebral blood flow, therefore uncoupling cerebral blood flow and rCMRO₂, but its effects on baseline CBV, SO₂, and rCMRO₂ remain controversial (Chen and Parrish, 2009; Perthen *et al*, 2008). Ventilation modes are also suspected to affect brain hemodynamics, although results are still inconsistent (Milan *et al*, 2009).

Combined FDNIRS and DCS offers an effective and quantitative bedside method to monitor CBV, SO₂, and BF_{ix} as well as rCMRO₂ in the premature brain. Quantitative values facilitate both individual follow-up and comparison among patients. Blood flow index and rCMRO₂ appear to be more accurate biomarkers of newborn brain development than SO₂.

Acknowledgements

The authors thank all the families for their participation in this study and the nurses, physicians, and staff in the Neonatal ICU, the Special Care Nursery, Pediatric Neurology, and the maternity units at Massachusetts General Hospital, Brigham and Women's Hospital and Children's Hospital Boston for helping with recruitment and data collection. In particular, the authors thank Marcia Kocienski-Filip, Maddy Artunduaga, Elizabeth A Warren, Sarah M Barnett, Kalpathy S Krishnamoorthy, Linda J Van Marter, Robert M Insoft, Jonathan H Cronin, Julianne Mazzawi, and Steven A Ringer. The authors also

thank David A Boas for his advice regarding data analysis. The content is solely the responsibility of the authors and does not necessarily represent the official views of the National Center for Research Resources or the National Institutes of Health.

Disclosure/conflict of interest

The authors declare no conflict of interest.

References

- André M, Lamblin MD, d'Allest AM, Curzi-Dascalova L, Moussalli-Salefranque F, Nguyen The Tich S, Vecchierini-Blineau MF, Wallois F, Walls-Esquivel E, Plouin P (2010) Electroencephalography in premature and full-term infants. Developmental features and glossary. *Neurophysiol Clin* 40:59–124
- Bassi L, Ricci D, Volzone A, Allsop JM, Srinivasan L, Pai A, Ribes C, Ramenghi LA, Mercuri E, Mosca F, Edwards AD, Cowan FM, Rutherford MA, Counsell SJ (2008) Probabilistic diffusion tractography of the optic radiations and visual function in preterm infants at term equivalent age. *Brain* 131:573–82
- Boas DA, Campbell LE, Yodh AG (1995) Scattering and imaging with diffusing temporal fields correlations. *Phys Rev Lett* 75:1855–8
- Boas DA, Yodh AG (1997) Spatially varying dynamical properties of turbid media probed with diffusing temporal light correlation. *J Opt Soc Am* 14:192–215
- Bourgeois J-P, Jastreboff PJ, Rakic P (1989) Synaptogenesis in visual cortex of normal and preterm monkeys: evidence for intrinsic regulation of synaptic overproduction. *Proc Natl Acad Sci* 86:4297–301
- Buckley EM, Cook NM, Durduran T, Kim MN, Zhou C, Choe R, Yu G, Shultz S, Sehgal CM, Licht DJ, Arger PH, Putt ME, Hurt HH, Yodh AG (2009) Cerebral monitoring in preterm infants during positional intervention measured with diffuse correlation spectroscopy and transcranial Doppler ultrasound. *Opt Express* 17:12571–81
- Carp SA, Dai GP, Boas DA, Franceschini MA, Kim YR (2010) Validation of diffuse correlation spectroscopy measurements of rodent cerebral blood flow with simultaneous arterial spin labeling MRI; towards MRI-optical continuous cerebral metabolic monitoring. *Biomed Opt Exp* 1:553–65
- Chen Y, Parrish TB (2009) Caffeine's effects on cerebrovascular reactivity and coupling between cerebral blood flow and oxygen metabolism. *NeuroImage* 44:647–52
- Cheung C, Culver JP, Kasushi T, Greenberg JH, Yodh AG (2001) *In vivo* cerebrovascular measurement combining diffuse near-infrared absorption and correlation spectroscopies. *Phys Med Biol* 46:2053–65
- Culver JP, Durduran T, Cheung C, Furuya D, Greenberg JH, Yodh AG (2003) Diffuse optical measurement of hemoglobin and cerebral blood flow in rat brain during hypercapnia, hypoxia and cardiac arrest. *Adv Exp Med Biol* 23:293–8
- de Alarcón P, Werner E (eds). (2005) *Neonatal Hematology*. UK: Cambridge University Press
- Dehaes M, Grant PE, Sliva D, Roche-Labarbe N, Pienaar R, Boas D, Franceschini M, Selb J (2011) Assessment of the frequency-domain multi-distance method to evaluate the brain optical properties: Monte Carlo simulations from neonate to adult. *Biomed Opt Express* 2:552–67
- Durduran T, Burnett MG, Yu G, Zhou C, Furuya D, Yodh AG, Detre JA, Greenberg JH (2004) Spatiotemporal quantification of cerebral blood flow during functional activation in rat somatosensory cortex using laser-speckle flowmetry. *J Cereb Blood Flow Metab* 24:518–25
- Durduran T, Zhou C, Buckley EM, Kim MN, Yu G, Choe R, Gaynor JW, Spray TL, Durning SM, Mason SE, Montenegro LM, Nicolson SC, Zimmerman RA, Putt ME, Wang J, Greenberg JH, Detre JA, Yodh AG, Licht DJ (2010) Optical measurement of cerebral hemodynamics and oxygen metabolism in neonates with congenital heart defects. *J Biomed Opt* 15:037004
- Edwards AD, Richardson C, Cope M, Wyatt JS, Delpy DT, Reynolds EOR (1988) Cotside measurement of cerebral blood flow in ill infants by near-infrared spectroscopy. *Lancet* 332:770–1
- Fantini S, Franceschini M, Maier JS, Walker SA, Barbieri B, Gratton E (1995) Frequency-domain multichannel optical detector for non-invasive tissue spectroscopy and oximetry. *Opt Eng* 34:34–42
- Fonta C, Imbert M (2002) Vascularization in the primate visual cortex during development. *Cereb Cortex* 12:199–211
- Franceschini M, Fantini S, Paunescu LA, Maier JS, Gratton E (1998) Influence of a superficial layer in the quantitative spectroscopic study of strongly scattering media. *Appl Opt* 37:7447–58
- Franceschini MA, Thaker S, Themelis G, Krishnamoorthy KK, Bortfeld H, Diamond SG, Boas DA, Arvin K, Grant PE (2007) Assessment of infant brain development with frequency-domain near-infrared spectroscopy. *Ped Res* 61:546–51
- Grant PE, Roche-Labarbe N, Surova A, Themelis G, Selb J, Warren EK, Krishnamoorthy KS, Boas DA, Franceschini MA, Grant PE (2009) Increased cerebral blood volume and oxygen consumption in neonatal brain injury. *J Cereb Blood Flow Metab* 29:1704–13
- Greisen G (2006) Is near-infrared spectroscopy living up to its promises? *Semin Fetal Neonatal Med* 11:498–502
- Huang L, Ding H, Hou X, Zhou C, Wang G, Tian F (2004) Assessment of the hypoxic-ischemic encephalopathy in neonates using non-invasive near-infrared spectroscopy. *Physiol Meas* 25:749–61
- Huppi PS, Warfield S, Kikinis R, Barnes PD, Zientara GP, Jolesz FA, Tsuji MK, Volpe JJ (1998) Quantitative magnetic resonance imaging of brain development in premature and mature newborns. *Ann Neurol* 43:224–35
- Li J, Dietsche G, Iftime D, Skipetrov SE, Maret G, Elbert T, Rockstroh B, Gisler T (2005) Noninvasive detection of functional brain activity with near-infrared diffusing-wave spectroscopy. *J Biomed Opt* 10:044002
- Milan A, Freato F, Vanzo V, Chiandetti L, Zaramella P (2009) Influence of ventilation mode on neonatal cerebral blood flow and volume. *Early Hum Dev* 85:415–9
- Nagy Z, Lagercrantz H, Hutton C (2010) Effects of preterm birth on cortical thickness measured in adolescence. *Cereb Cortex PMID* 21:300–6
- Naulaers G, Cossey V, Morren G, Van Huffel S, Casaer P, Devlieger H (2004) Continuous measurement of cerebral blood volume and oxygenation during rewarming of neonates. *Acta Paediatr* 93:1540–2
- Nicklin SE, Hassan IA-A, Wickramasinghe YA, Spencer SA (2003) The light still shines, but not that brightly? The current status of perinatal near infrared spectroscopy. *Arch Dis Child Fetal Neonatal Ed* 88:263–8

- Patel J, Marks K, Roberts I, Azzopardi D, David EA (1998) Measurement of cerebral blood flow in newborn infants using near infrared spectroscopy with indocyanine green. *Ped Res* 43:34–9
- Perthen JE, Lansing AE, Liao J, Liu TT, Buxton RB (2008) Caffeine-induced uncoupling of cerebral blood flow and oxygen metabolism: a calibrated BOLD fMRI study. *NeuroImage* 40:237–47
- Petrova A, Mehta R (2006) Near-infrared spectroscopy in the detection of regional tissue oxygenation during hypoxic events in preterm infants undergoing critical care. *Pediatr Crit Care Med* 7:449–54
- Roche-Labarbe N, Carp SA, Surova A, Patel M, Boas DA, Grant PE, Franceschini MA, Roche-Labarbe N (2010) Noninvasive optical measures of CBV, StO₂, CBF index, and rCMRO₂ in human premature neonates' brains in the first six weeks of life. *Hum Brain Mapp* 31:341–52
- Smyser CD, Inder TE, Shimony JS, Hill JE, Degnan AJ, Snyder AZ, Neil JJ (2010) Longitudinal analysis of neural network development in preterm infants. *Cereb Cortex* 20:2852–62
- Takahashi T, Shirane R, Sato S, Yoshimoto T (1999) Developmental changes of cerebral blood flow and oxygen metabolism in children. *Am J Neuroradiol* 20:917–22
- Tina LG, Frigiola A, Abella R, Artale B, Puleo G, D'Angelo S, Musmarra C, Tagliabue P, Li Volti G, Florio P, Gazzolo D (2009) Near infrared spectroscopy in healthy preterm and term newborns: correlation with gestational age and standard monitoring parameters. *Curr Neurovasc Res* 6:148–54
- Toet MC, Flinterman A, van de Laar I, de Vries JW, Bennink GBWE, Uiterwaal CSPM, van Bel F (2005) Cerebral oxygen saturation and electrical brain activity before, during, and up to 36 hours after arterial switch procedure in neonates without pre-existing brain damage: its relationship to neurodevelopmental outcome. *Exp Brain Res* 165:343–50
- Wolf M, Greisen G (2009) Advances in near-infrared spectroscopy to study the brain of the preterm and term neonate. *Clin Perinatol* 36:807–34
- Wolthuis R, van Aken M, Fountas K, Robinson JSJ, Bruining HA, Puppels GJ (2001) Determination of water concentration in brain tissue by Raman spectroscopy. *Anal Chem* 73:3915–20
- Wray S, Cope M, Delpy DT, Wyatt JS, Reynolds EO (1988) Characterization of the near infrared absorption spectra of cytochrome aa3 and haemoglobin for the non-invasive monitoring of cerebral oxygenation. *Biochim Biophys Acta* 933:184–92
- Wyatt JS, Cope M, Delpy DT, Wray S, Reynolds EO (1986) Quantification of cerebral oxygenation and haemodynamics in sick newborn infants by near infrared spectrophotometry. *Lancet* 2:1063–6
- Zhao J, Ding HS, Hou XL, Zhou CL, Chance B (2005) *In vivo* determination of the optical properties of infant brain using frequency-domain near-infrared spectroscopy. *J Biomed Opt* 10:024028



This work is licensed under the Creative Commons Attribution-NonCommercial-No Derivative Works 3.0 Unported License. To view a copy of this license, visit <http://creativecommons.org/licenses/by-nc-nd/3.0/>

Supplementary Information accompanies the paper on the Journal of Cerebral Blood Flow & Metabolism website (<http://www.nature.com/jcbfm>)